Accepted Manuscript online: 2022-08-08 Article published online: 2022-11-27

Differential Diagnosis of Keratoconus Based on New Technologies

Differenzialdiagnose des Keratokonus basierend auf neuen Technologien

Authors
Haris Sideroudi, Elias Flockerzi, Berthold Seitz

Affiliation
Department of Ophthalmology, Saarland University Medical Center and Saarland University Faculty of Medicine, Homburg/Saar, Germany

Key words
keratoconus, pellucid marginal degeneration, keratoglobus, posterior keratoconus, Fuchs Terrien marginal degeneration, differential diagnosis

Schlüsselwörter
Keratokonus, pelluzide marginale Degeneration, Keratoglobus, posteriorer Keratokonus, Fuchs-Terrien'sche marginale Hornhautdegeneration, Differenzialdiagnose

received	22. 12. 2021
accepted	30. 7. 2022
published online	27. 11. 2022

Bibliography
Klin Monatsbl Augenheilkd 2023; 240: 57–72
DOI 10.1055/a-1920-6929
ISSN 0023-2165
© 2022. Thieme. All rights reserved.
Georg Thieme Verlag KG, Rüdigerstraße 14, 70469 Stuttgart, Germany

Correspondence
Dr. Haris Sideroudi, PhD
Department of Ophthalmology, Saarland University Medical Center and Saarland University Faculty of Medicine
Kirrberger Str. 100, 66421 Homburg, Germany
Phone: + 30 69 36 72 70 76, Fax: + 30 6 84 11 62 24 79
haris.sideroudi@uks.eu

ABSTRACT

Keratoconus (KC) must be distinguished from other corneal ectatic diseases and thinning disorders for stage-appropriate and suitable management of each condition. The most relevant corneal pathologies that may imitate the tomographic KC pattern are pellucid marginal degeneration (PMD), keratoglobus, posterior keratoconus, and Fuchs-Terrien marginal degeneration (FTMD). In moderate cases of KC, differentiation is typically possible using slit lamp examination and corneal tomography with evaluation of the location of the corneal thinning region. In early cases, however, differential diagnosis may be more challenging since the cornea may look relatively normal. In severe cases, the extended area of corneal thinning also complicates differentiation. Biomicroscopic findings cannot always give all the information needed to distinguish KC from related ectatic corneal conditions. The aim of this work is to discuss contemporary techniques and findings to assist physicians to identify the correct diagnosis. Corneal topography has been used in recent decades as the main tool for imaging in ectatic corneal diseases. Moreover, Scheimpflug cameras (corneal tomographers), which analyze both anterior and posterior corneal surfaces, curvatures, pachymetry, elevation data, higher order aberrations, Fourier analysis of keratometric data, and corneal density have become the most promising tools for diagnosis and follow-up of ectatic diseases. A noninvasive air pulse tonometer in conjunction with an ultrahigh-speed Scheimpflug camera complements tomographic findings by analyzing biomechanical corneal properties. A confocal microscopy system, which is a novel clinical technique for the study of corneal cellular structure, could contribute effectively in the same direction. Moreover, anterior segment optical coherence tomography (AS-OCT) creates cross-sections, which can be generated into a three-dimensional structure to produce corneal epithelial thickness (ET) measurements. ET mapping is increasingly recognized as a sensitive tool for the diagnosis of ocular surface disorders. Combining information of all these systems could lead to a more effective identification and differential diagnosis of ectatic corneal disorders.

ZUSAMMENFASSUNG

Die Unterscheidung zwischen Keratokonus (KK) und anderen ektatischen Hornhauterkrankungen ist für eine angemessene Behandlung der jeweiligen Erkrankung unerlässlich. Die wichtigsten Hornhautpathologien, die bei der Differenzialdiagnose des KK in Betracht gezogen werden müssen, sind die pelluzide marginale Degeneration (PMD), der Keratoglobus, der posteriore Keratokonus und die Fuchs-Terrien'sche marginale De-

This document was downloaded for personal use only. Unauthorized distribution is strictly prohibited.

generation (FTMD). In mittelschweren KK-Fällen ist die Differenzierung aufgrund der klassischen Lage der Hornhautverdünnungsregion möglich. In frühen Fällen ist die Differenzialdiagnose jedoch schwierig, da die Hornhaut relativ normal aussehen kann. In fortgeschrittenen Stadien hingegen ist die Differenzierung aufgrund des ausgedehnten Bereichs der Hornhautverdünnung mitunter ebenfalls schwierig. Biomikroskopische Befunde können nicht alle Informationen liefern, die zur Unterscheidung des KK von anderen ektatischen Hornhauterkrankungen erforderlich sind. Daher werden moderne Techniken und Befunde diskutiert, um die richtige Differenzialdiagnose sicherstellen zu können. Hornhauttopografiekarten wurden in den letzten Jahrzehnten als Hauptinstrument für die bildgebende Differenzialdiagnose verwendet. Darüber hinaus wurden Scheimpflug-Kameras (Hornhauttomografen), die sowohl die vordere als auch die hintere Hornhautfläche anhand von Krümmungsdaten, Pachymetrie, Elevationsmessungen, Aberrationen höherer Ordnung, Fourier-Analysen keratometrischer Daten und die Hornhautdichte analysieren, zum wichtigsten Instrument für die Diagnose und Verlaufskontrolle ektatischer Hornhauterkrankungen. Seit neuestem zeichnet ein nicht invasives Luftstoßtonometer in Verbindung mit einer Ultrahochgeschwindigkeits-Scheimpflug-Kamera die Reaktion der Hornhaut auf diesen mechanischen Stimulus auf und analysiert so ihre biomechanischen Eigenschaften. Des Weiteren könnte die konfokale Mikroskopie effektiv zur Differenzialdiagnose beitragen. Darüber hinaus erzeugt die optische Kohärenztomografie des vorderen Segments (AS-OCT) Querschnitte, die in eine 3-dimensionale Struktur umgewandelt werden können, um die Hornhautepitheldicke zu messen. Das Endothel-Mapping wird zunehmend als wirksames Instrument für die Diagnose von Erkrankungen der Augenoberfläche anerkannt. Die Kombination der Informationen all dieser Systeme könnte eine umfassendere Identifizierung und Differenzialdiagnose ektatischer Hornhauterkrankungen ermöglichen.

Keratoconus and Other Related Ectatic Corneal Diseases

Keratoconus

Keratoconus (KC) is a progressive corneal ectasia that is characterized by irregular myopic astigmatism, paracentral stromal thinning, and apical corneal protrusion that may eventually result in scarring and, in mild to considerable impairment, in the quality of vision [1]. Although it may start in one eye, it is considered a bilateral condition [1]. KC involves the central two-thirds of the cornea, and the cone is usually localized just below the visual axis (▸ **Fig. 1** and **2**) [2]. The area of conical protrusion is usually surrounded by a superficial iron ring called the Fleischer ring. High irregular astigmatism may occur because of scars and lined posterior folds, so-called Vogt striae. The development of a conical shape can occur in the presence of multiple clinical settings or, more commonly, it can occur without any known associated condition.

KC usually starts at puberty and progresses until it stabilizes in the 3rd or 4th decade. KC severity has been found to present an inverse correlation with age [3]. The earlier the onset of KC, the more severe the clinical phenotypes.

KC appears in all ethnicities; the prevalence in studies is reported to range from 0.0003% in Russia to 2.3% in central India [4]. Higher incidence rates were detected in New Zealand and the Asir province in Saudi Arabia [4]. The most commonly cited prevalence is 0.054% and was raised in Minnesota (USA) by Kennedy et al. who diagnosed KC based on scissors movement on retinoscopy and keratometry [5]. These varying incidences in different studies could be partially explained by the diagnostic method, genetics, nutritional, or environmental factors and the high UV exposure of their population [4]. Moreover, concerning gender distribution, recent studies reported a preponderance of males up to 73% [6].

There are three signs that typically characterize KC histopathologically: (1) Stromal corneal thinning, (2) Bowman's layer breaks, and (3) Iron deposits within the corneal epithelium's basal layer [1]. Epithelial thinning is the most common pathology observed among the KC corneas followed by breaks in Bowman's layer. Bowman's layer plays an important role in strengthening the cornea. Damage to or loss of Bowman's layer results in the reduction of corneal rigidity and therefore contributes to KC pathogenesis. The breaks in Bowman's layer are filled with epithelium or proliferating collagenous tissue that is derived from the anterior stroma [6].

Pellucid marginal degeneration: keratotorus

Pellucid marginal degeneration (PMD) is a no-inflammatory and progressive ectatic disorder that typically affects the inferior peripheral cornea leading to a corresponding steepening and thinning (▸ **Fig. 1** and **2**). The characteristic finding is a narrow band of corneal thinning, 1 to 2 mm in width, parallel to the inferior limbus. The area between the thinned section and the limbus is typically unaffected up to moderate stages. High "against-the-rule" astigmatism is a result due to the corneal protrusion above the area of thinning. The cornea superior to the band of thinning is of normal thickness and has the most marked anterior displacement just above the band. The magnitude of the resulting astigmatism depends on the location where it is measured. Superior to the thinning area, the vertical meridian flattens and causes the appearance of "against-the-rule astigmatism" up to 20 D [7].

PMD is usually detected between the 2nd and 5th decade of life. There is neither evidence that PMD is genetically inherited nor are there associations to one gender. However, moderate or high astigmatism has been found in family members without further associated symptoms [8]. Moreover, there is no established link of PMD, neither with a specific gene nor with systematic or other ocular clinical conditions.

This document was downloaded for personal use only. Unauthorized distribution is strictly prohibited.

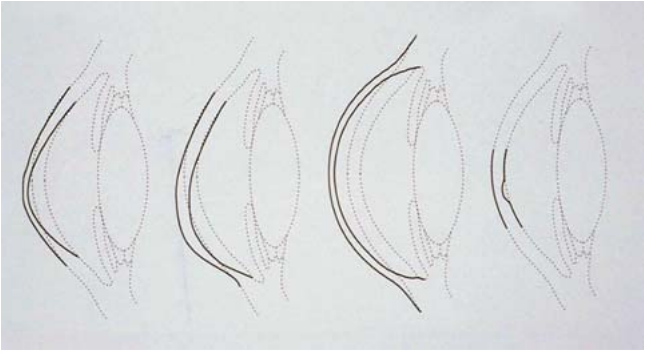

▶ **Fig. 1** Typical appearance of thinning in keratoconus, pellucid marginal degeneration, keratoglobus, posterior keratoconus, and Fuchs-Terrien marginal degeneration.

Histopathological evidence showed an absent Bowman's layer, a normal epithelium distribution, and increased mucopolysaccharide deposition within the corneal stroma [9].

Keratoglobus

Keratoglobus is a bilateral generalized thinning and global protrusion of the cornea, which is often more pronounced in the periphery. The thinning reaches down to 20% of normal corneal thickness. The cornea is transparent without deposits, unless there are acute conditions such as a corneal hydrops or chronic conditions, for example, scarring in severe cases (▶ **Fig. 1**).

Keratoglobus usually has its onset at birth and there is no progression over time. The exact genetics of the disorder are not yet fully understood. However, keratoglobus is considered to be an autosomal recessive disorder and it has been associated with disorders of the connective tissue, such as Ehlers-Danlos syndrome, Marfan syndrome, and Rubinstein-Taybi syndrome [10]. Moreover, keratoglobus may be associated with a bluish sclera appearance, which is considered to be a manifestation of Ehlers-Danlos syndrome or Marfan syndrome [11].

Histopathological evidence showed an absence of Bowman's layer, breaks or thickening of the Descemet membrane, and a stromal thinning, mainly in the periphery. Epithelial hyperplasia has also been reported in some cases [12]. Immunohistochemical studies showed decreased levels of proteinase inhibitor alpha-1 and increased expression of the transcription factor Sp1 in the corneal epithelial cells. Moreover, there was an increased level of matrix metalloproteinases (MMPs) 1, 2, and 3 within the epithelial cells diffusely throughout the cornea, with a maximum level at the midperiphery corresponding to the areas of Bowman's layer disruptions. These alterations are very similar to those seen in advanced KC and have brought concerns about whether the disorders comprising this group are separate clinical entities or rather part of a spectrum of the same disease process. In fact, the histological similarities have led to the speculation that keratoglobus may be an end-stage manifestation of advanced KC [12].

Another main characteristic of keratoglobus is the increased risk of corneal rupture after minimal trauma. Theoretically, the amount of stress on the corneal tissue is directly proportional to the radius of curvature and inversely proportional to the corneal thickness. Compared to other ectatic diseases, keratoglobus presents a greater radius of curvature at equal thickness. Consequently, the combination of higher corneal stress and a minimal level of trauma may increase the incidence of corneal rupture [13].

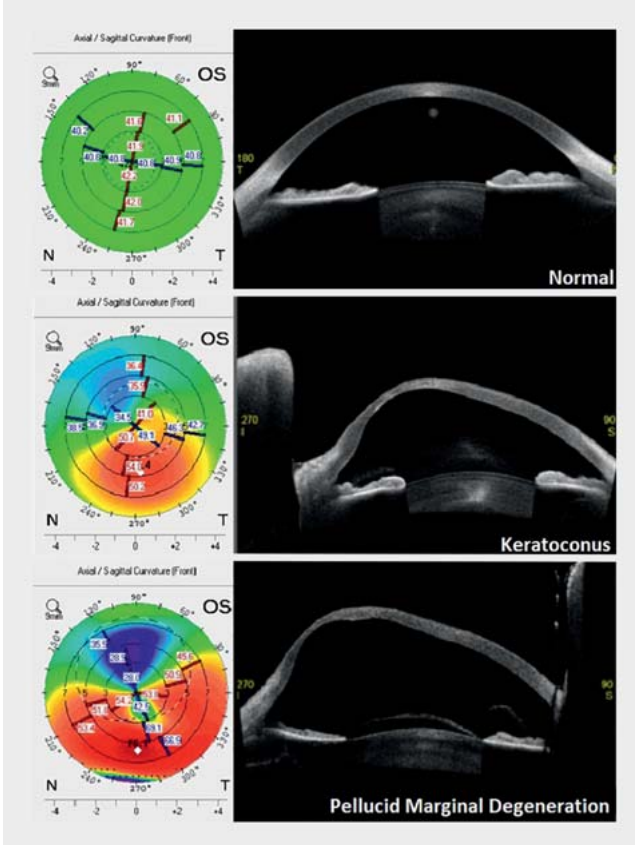

▶ **Fig. 2** Corneal tomography and anterior segment OCT in normal keratoconus and pellucid marginal degeneration patients.

Posterior keratoconus

Posterior KC is a rare nonprogressive and noninflammatory corneal disorder with an abnormal increment of posterior corneal curvature. It is classified mainly in two subtypes: the KC posticus generalis, which affects the entire posterior corneal curvature, and the KC posticus circumscriptus, with a localized and usually para-central protrusion of the posterior part of the cornea (▶ **Fig. 1**) [14]. KC posticus generalis is characterized by an increase of the entire posterior corneal curvature, whilst the cornea usually remains clear. KC posticus circumscriptus is a posterior corneal indentation localized in the central or paracentral area with an associated stromal scarring or opacity. In both cases, the anterior cornea remains intact without abnormal steepening or irregularities. The thinning could be up to 1/3 of normal corneal thickness. Since the refractive index of the aqueous humor (n = 1.336) and cornea (n = 1.377) are only slightly different, the changes of curvatures in the posterior cornea present inferior optical consequences compared to equal changes in the anterior corneal surface.

This document was downloaded for personal use only. Unauthorized distribution is strictly prohibited.

Among family members, posterior KC may present an autosomal dominant mode of inheritance and it has been associated with systemic abnormalities. The most common are sclerosis, cleavage anomalies, aniridia, ectropion uveae, iris atrophy, glaucoma, lenticonus anterior, ectopia lentis, and anterior lens opacities. Despite the systemic associations, no genetic locus has been identified yet [15].

The onset of the disease is supposed to be prior to 8 months of gestation. Histological and transmission electron microscopy analysis showed a disorganized irregular Descemet membrane and widely spaced collagen with an abnormal banding and multilaminar configuration in the thinned zone. Bowman's layer may be absent centrally, replaced by a random arrangement of collagen and scattered fibroblasts. Moreover, the epithelial basement membrane is usually partially absent with a disruption of the basal epithelium. Despite the presence of guttae, the surrounding endothelium seems to be intact [16].

Fuchs-Terrien marginal degeneration

Fuchs-Terrien marginal degeneration (FTMD) is a rare bilateral ectatic corneal disease with slow progression. Although it is typically noninflammatory, a variant characterized by prominent inflammation exists [17, 18]. The degeneration typically begins superiorly and progresses circumferentially (▶ **Fig. 1**). It usually presents a marginal opacification and a superficial vascularization with characteristic furrow formation of the peripheral cornea in the otherwise clear area between the opacification and the limbus. This "gutter-like furrow" does not ulcerate; however, lipid deposition occurs at the leading edge of the affected area [19]. There is a regional corneal flattening due to the peripheral thinning at the beginning of the disease. However, the superior and/or inferior thinning of the peripheral cornea may result in a large "against-the-rule" oblique astigmatism [17].

FTMD affects mainly males in their mid-twenties [18]. It has been associated with systemic disorders such as arthritis [19] and recently with Meibomian gland dysfunction [17]. However, since there are many FTMD patients without an underlying systemic disease, an association with systemic diseases remains questionable.

Histopathological examination and transmission electron and light microscopy show pycnotic nuclei and vacuole formation within epithelial cells [17]. There is also a thickened basement membrane and fragments in Bowman's layer [17]. Moreover, the number of lamellae in the stroma is decreased due to breaks and degradation of collagen fibrils. A thickening of the Descemet membrane also occurs and shows signs of previous breaking and healing with attachment of normal or degradative endothelial cells. Various types of cells have been found in the layers of the cornea such as histocytes, lymphocytes, fibrocytes, plasma cells, and even blood vessels [17].

Daily Routine Examination and New Technologies

Slit lamp examination

Typical clinical KC signs visible at slit lamp examination comprise the Fleischer ring, Vogt striae, and paracentral corneal thinning with conical protrusion. Subepithelial fibrillary lines, prominent nerves, and scarring of Bowman's layer can also be detected [20].

These findings are rarely present in PMD cases, thus constituting a differential factor to discriminate between both diseases, mostly in moderate and advanced cases. PMD corneas typically show a band of stromal thinning from the 4 to the 8 o'clock position in proximity of the limbus. Moreover, unlike KC, no obvious cone or lipid deposition is recognized during clinical examination in PMD cases.

Keratoglobus is typically not associated with Vogt striae, Fleischer ring, or corneal scarring, and ruptures of Descemet's membrane or development of an acute hydrops are less common than in KC. Patients with keratoglobus are very likely to present corneal ruptures caused by minimal trauma, but often, there is no antecedent history of trauma in their medical history. However, corneal perforations and/or ruptures are rare findings in KC, even in cases of a corneal hydrops.

Slit lamp photographs of posterior KC show circumscribed or extended protrusion of the posterior corneal curvature with a concomitant stromal thinning and an intact anterior corneal surface. Although the Fleischer ring and scarring may be present in both, KC and posterior KC, the characteristic signs of posterior KC upon slit lamp examination are localized stromal opacities, which are present even in very early stages [21].

FTMD presents a characteristic peripheral superior thinning, whereas the highest protrusion in KC is centrally or slightly inferior. Further characteristics include a furrowing of the peripheral cornea with associated lipid deposition and vascularization. Lipid deposition occurs along the anterior edge while vascularization is mainly observed within the anterior stroma growing radially from the limbus. In early stages, these changes include a fine, whitish or yellow, punctate, stromal opacification that may resemble an incomplete arcus lipoides [18]. These findings have not been reported in KC cases.

Corneal topography and tomography

Corneal topographers are used to characterize the shape of the cornea creating axial power maps, similar to how one would characterize a mountain using a topographic map. Originally, corneal topography was only used to describe the anterior surface of the cornea. Nowadays, devices can analyze both the anterior and posterior corneal surfaces, creating a three-dimensional corneal tomography map. Advances in digital photography and computer processing have vastly increased the utility of these so-called corneal tomographers. Corneal tomographers are state-of-the-art instruments today and, therefore, essential for the diagnosis of KC and other ectatic corneal disorders.

Most eyes with KC show a slight paracentral or inferior steepening pattern in the axial power map, while eyes with PMD show

This document was downloaded for personal use only. Unauthorized distribution is strictly prohibited.

a crab claw pattern (▶ **Fig. 2**). However, it has been reported that the crab claw pattern is not a reliable diagnostic criterion for PMD because it is also seen in eyes with inferior KC [22].

Detailed examinations of the anterior and posterior corneal axial maps in KC, PMD, and normal cases could provide valuable information aiming to finally establish a topographic borderline between both diseases. Specifically, the axial power maps were found to present eight patterns: round, oval, symmetric bow tie, asymmetric bow tie, central steepening, lazy 8 figure, inferior steepening, and crab claw appearance [23].

In controls, the round pattern was the most common. A classic topographic pattern of KC presents a well-delimited zone with a high dioptric value, surrounded by progressively decreasing curvature zones. The corneal protrusion is normally conical, circular, or oval and it is mainly located in the center of the cornea or slightly inferiorly displaced. Moreover, the corneal protrusion may also be manifested in an asymmetric bow tie pattern. The most frequent anterior topographic patterns in eyes with KC were found to be the inferior steepening pattern followed by the central steepening pattern (▶ **Table 1**) [23].

PMD presents a very characteristic corneal topographic pattern, the "crab claw" pattern (▶ **Fig. 2**), which is also called "butterfly", "lobster". or "kissing doves" [24]. This typical pattern appears due to flattening of the vertical meridian above the thinning band, which generates a marked "against-the-rule" astigmatism. Hence, the most common anterior topographic pattern in eyes with PMD is the crab claw pattern followed by the inferior steepening pattern (▶ **Table 1**) [23].

Keratoglobus usually presents with irregular astigmatism and an irregular power distribution similar to KC. However, the steepening is generalized in the whole cornea, referring to both anterior and posterior curvatures. In addition, unlike KC, there is a peripheral arc of increased power resulting in flattening of the "arching" of the bow tie configuration in the topography [25].

In KC posticus generalis, there is a general uniform posterior corneal steepening, and this is a differential factor from KC. There could even be anterior abnormalities [26]. In KC posticus circumscriptus, surface topography showed a corneal steepening over the affected area. If the affected area is in the superior, nasal, or temporal corneal quadrant, the differential diagnosis is clear. However, if the affected corneal area is in the inferior corneal quadrant, the differentiation between these two clinical entities becomes more difficult [26].

In FTMD, the topography map is characterized by flattening in the area of peripheral thinning caused by the disease. The peripheral furrowing, which typically begins superiorly and/or inferiorly, leads to a flattening of the vertical meridian, thus resulting in the characteristic "against-the-rule" astigmatism. This common pattern results out of the preferential involvement of the superior and/or inferior peripheral cornea. In some patients, the central corneal topography may remain relatively spherical if the area of thinning is small or if the disorder extends around the entire circumference of the cornea [17–19]. In contrast, the steep axis occurs in 90-degree geometry in the majority of KC cases.

▶ **Table 1** Classification of eyes in the axial power map according to topographic pattern [23].

Topographic pattern in axial power map	KC	PMD (%)	Control
Round	0	0	58
Oval	0	0	11
Symmetric bow tie	0	0	26
Asymmetric bow tie	0	2	4
Central steepening	24	2	0
Lazy 8	8	0	0
Inferior steepening	67	18	0
Crab claw	2	78	0
Total	100	100	100

Pachymetric data

A full pachymetric map of the cornea can be generated using corneal cross-section analysis. Scanning slit imaging, Scheimpflug imaging, and AS-OCT can generate pachymetric maps. As KC is characterized by a focal and progressive thinning, a full pachymetric map may be able to identify KC cases with normal or irregular tomographies. Previous studies have reported successful identification of KC when using pachymetric screening parameters [27].

Advanced PMD cases are characterized by the presence of a maximum thinning in the inferior cornea, with a progressive increase of the thickness through central and superior areas. The mean central corneal thickness (CCT) and thinnest corneal pachymetry (TCP) in the PMD group were found to be higher compared to the KC group and lower than in the normal group. This indicates that the magnitude of the corneal thinning is not as prominent in PMD and may not be a diagnostic factor. As expected, the location of the TCP is more inferior compared to the location in the KC group [23, 27, 28].

Furthermore, the pachymetric maps can be classified into six patterns: central round, central oval, paracentral round, paracentral oval, decentered round, and decentered oval [23]. The term "central" was used when the location of the TCP point was located within the central 2-mm diameter zone. When the TCP point was beyond this 2-mm-diameter zone and within a 3-mm diameter zone, the map was considered to be paracentral; if it fell outside the 3-mm diameter zone, the map was classified as decentered [23].

The most common pachymetry pattern in eyes with PMD was the decentered oval pattern followed by a decentered round pattern. In contrast, neither the decentered oval nor the decentered round patterns were seen in KC and normal eyes. In eyes with KC, the most frequent pachymetry pattern was a central round pattern followed by the paracentral round pattern [23]. The distribution of pachymetric map patterns for the three groups of eyes is shown in ▶ **Table 2**. A pachymetry map may reveal characteristic signs of PMD and may thus contribute mainly to the decision in a differential diagnosis between KC and PMD, especially when a

This document was downloaded for personal use only. Unauthorized distribution is strictly prohibited.

▶ **Table 2** Classification of eyes in the pachymetric map according to topographic pattern [23].

Topographic pattern in the pachymetric map	PMD (%)	KC (%)	Control (%)
Central round	14	51	96
Central oval	8	18	0
Paracentral round	18	27	4
Paracentral oval	12	4	0
Decentered round	20	0	0
Decentered oval	27	0	0
Total	100	100	100

similar pattern is present in topographic maps for both diseases [28]. However, it is well known that the peripheral stromal dilution in PMD is very difficult to detect and peripheral measurements are not captured and interpolated by the software. In such cases, the use of manual pachymetric measurements of images or corneal tomographers with better segmentation algorithm, which ensure limbus-to-limbus tracing of the corneal surface, seemed to be a more reliable method for evaluating corneal thickness in PMD [29].

Keratoglobus is characterized by a diffuse thinning and global protrusion. It may be distinguished from KC based on the thinning area, which is extensively present over the entire corneal surface while KC affects only a central or paracentral region.

Posterior KC usually presents a central or paracentral corneal thinning coinciding with the localized excavation of the posterior surface. Like in typical KC, the pachymetric patterns could have a central or paracentral round or oval formation in KC posticus circumscriptus. Hence, there is no differential sign based solely on pachymetric maps in these cases. Keratoconus posticus generalis presents a diffuse thinning of the entire corneal surface. We could assume that a pachymetric pattern has more similarities with keratoglobus than with KC.

Pachymetric maps in FTMD present a peripheral corneal thinning, which may extend to the midperiphery, but rarely to the central cornea. There is usually a significant thinning in the superior part of the cornea, which progresses circumferentially towards the inferior cornea. In this stage, the pachymetry map presents a ring-shaped pattern. At the final stage of the disease, the peripheral thinning area width increases towards the center. Hence, besides the clinical findings, a pachymetric map could be a useful instrument in differentiating between KC and FTMD.

Corneal elevation maps

These maps do not represent data directly measured by the corneal tomographer but are obtained by comparing the reconstruction of the anterior or posterior corneal surface to the best-fitted surface, typically a sphere, an ellipsoid, or a toroid. The difference between both surfaces is provided by height data that correspond to the elevation maps. These maps present several advantages: (1) data are presented quantitatively in µm, they are highly accurate, and they have a high sensitivity to small ectatic changes that can occur in the corneal morphology [30], and (2) corneal tomographers allow the selection of the best-suited surface to generate the elevation map, which results in a sensitivity increase in view of the clinical diagnosis [31]. These maps provide, for both the anterior and posterior corneal surfaces, the elevation of the corneal apex, the elevation at the TCP point, and the elevation of the central region, which have been proven to be very useful for the clinical diagnosis of and differentiation between ectatic corneal diseases.

Eyes with KC have increased values in anterior and posterior elevation maps [25, 31]. In the PMD group, the maximum elevation was higher for both anterior and posterior surfaces and was located more inferior than in healthy cases [27, 32].

Compared to KC, PMD presents significantly higher values for inferiorly located maximum elevation values for both anterior and posterior corneal surfaces [22].

Moreover, the elevation maps were categorized into nine patterns: central regular ridge, central irregular ridge, central incomplete ridge, central island, asymmetric regular ridge, asymmetric irregular ridge, asymmetric incomplete ridge, asymmetric island, and unclassified [23].

The majority of elevation patterns in PMD cases is the asymmetric island pattern in the anterior and posterior corneal surfaces (80 and 92%, respectively). The asymmetric island pattern was also the most common for both the anterior and posterior corneal surfaces in KC (37 and 41%, respectively), but with a lower incidence compared to PMD. KC also presents an asymmetric regular ridge with 24% incidence in the anterior corneal surface and 14% incidence in the posterior corneal surface. Moreover, the central island elevation pattern is highly frequent in KC in both the anterior (12%) and posterior corneal surfaces (20%). In PMD, there are no cases with a central island or asymmetric regular ridge (▶ **Table 3**) [23].

Keratoglobus presents high values in the elevation map in the total anterior and posterior corneal areas. Although the pattern seems to be normal, the values are significantly higher than in normal corneas. Unlike KC, the generalized and global protrusion does not create central or asymmetric islands in elevation maps.

In posterior KC, the anterior elevation map seems regular. However, there is a protrusion in the posterior elevation map. This pattern could also occur in some KC cases with a normal anterior elevation map and an irregular posterior elevation map. However, the anterior elevation map is already affected in early KC stages, while the abnormal elevation data is limited to the posterior corneal surface in posterior KC.

In FTMD, the anterior and posterior elevation maps showed a superotemporal paracentral elevation above the best-fit sphere since this pathology typically starts superiorly and spreads circumferentially.

Corneal higher-order aberrations

Wavefront aberrometers quantify whole eye optical errors compared to an unaberrated reference wavefront. The shape of the eye's wavefront error can be quantitatively described using a polynomial expansion. Zernike polynomials divide and analyze the wavefront into unique components. Higher-order aberrations

This document was downloaded for personal use only. Unauthorized distribution is strictly prohibited.

▶ **Table 3** Classification of eyes in the elevation map according to topographic pattern [23].

Topographic pattern in the elevation map	PMD		KC		Control	
	Anterior (%)	Posterior (%)	Anterior (%)	Posterior (%)	Anterior (%)	Posterior (%)
Central regular ridge	2	2	4	2	70	57
Central irregular ridge	2	2	2	0	11	38
Central incomplete ridge	0	0	0	4	9	4
Central island	0	0	12	20	0	0
Asymmetric regular ridge	2	0	24	14	0	0
Asymmetric irregular ridge	6	0	6	0	0	0
Asymmetric incomplete ridge	8	2	16	20	0	0
Asymmetric island	80	92	37	41	0	0
Unclassified	0	2	0	0	9	2
Total	100	100	100	100	100	100

(HOAs) include third-order and advancing higher Zernike modes, such as coma, trefoil, spherical aberrations, or quadrafoil. High levels of HOAs depend on pupil size and may have a detrimental effect on retinal image quality. This visual degradation occurs even in normal and, to a higher extent, in ectatic corneal diseases [33].

All of the anterior corneal aberration measurements are reported to be significantly higher in KC corneas than in normal corneas (▶ **Fig. 3**). The most sensitive HOAs seemed to be the primary spherical aberration, primary vertical coma, coma root mean square (RMS), and coma-like RMS [34].

Total HOAs, trefoil, coma, tetrafoil, and secondary astigmatism were reported to be higher in PMD corneas than in healthy controls [34].

HOAs also showed some differences in PMD compared to KC (▶ **Fig. 3**). The more peripherally localized ectasia in PMD results in a higher degree of trefoil, a third-order aberration that is located more peripherally in the Zernike pyramid table. In contrast, the more central third-order HOA, negative vertical coma, is characteristically severely elevated in KC. Aspherical aberration also has negative values in KC and positive values in most PMD cases. HOAs thus definitely show different patterns in PMD compared to KC corneas, possibly due to the difference in the position of the corneal apex relative to the pupil entrance [34].

Despite the fact that HOA maps present differences between PMD and KC, there is no strong evidence that they could be used as a standalone diagnostic tool to differentiate between those two diseases.

A different corneal shape due to different areas of corneal thinning and corneal topographic and tomographic appearances could be a reason for a different HOA profile between KC and keratoglobus, posterior KC, and FTMD. However, there are no scientific studies available in the literature to prove this hypothesis, yet.

Fourier analysis of topographic data

Fourier series are trigonometric sine and cosine functions with increasing periodicity and a function with a period of 2pi that can be transformed into a Fourier harmonic series as follows:

$$f(\varphi) = \sum [a_n \cos(n\varphi) + b_n \sin(n\varphi)]$$

This can be rewritten as a cosine function including a phase shift angle as follows:

$$f(\varphi) = \sum [c_n \cos n(\varphi + a_n)]$$

By performing Fourier series analysis in videokeratography data, it is possible to decompose circumferential fluctuations of the corneal power into various components that have a direct clinical correlation. The analysis actually decomposes the matrix of corneal refractive powers into four indices, such as spherical power, regular astigmatism, asymmetry, and higher-order irregularity.

The spherical equivalent and the regular astigmatic values are proportional to the keratometric spherical and astigmatic powers. The rest of the Fourier components have no keratometric equivalent, although they have a distinct clinical value. Decentration is a tilt of the cornea with respect to the axis of the videokeratoscope. Irregular astigmatism reflects a series of optical imperfections that degrade retinal image quality. A qualitative keratometric assessment of irregular astigmatism can be made based on mire quality. However, Fourier analysis can quantify irregular astigmatism as the sinusoidal variation in power (i.e., harmonics with $n > 2$) [35].

Significantly higher values were indicated for decentration, regular astigmatism, and irregularities for both anterior and posterior corneal surfaces, even in early KC stages compared to healthy corneas [35, 36]. These findings are in agreement with the qualitative interpretation of color-coded maps of videokeratography and Fourier analysis, since KC corneas usually show a

This document was downloaded for personal use only. Unauthorized distribution is strictly prohibited.

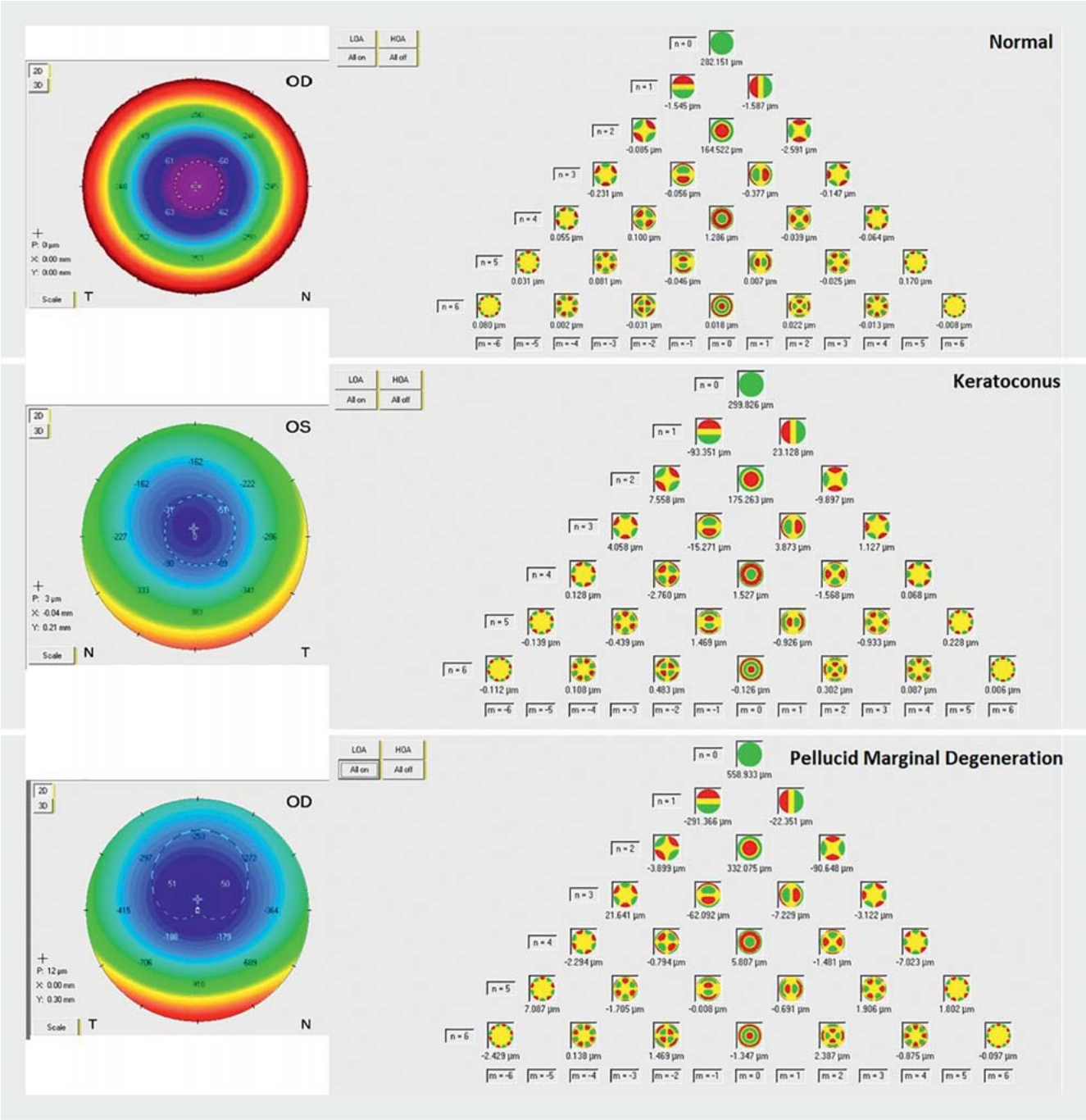

▶ **Fig. 3** Zernike vector analysis in normal, keratoconus, and pellucid marginal degeneration patients.

steeper curvature, higher astigmatism, higher asymmetry, and severe irregularity (▶ **Fig. 4**).

PMD corneas present with irregular astigmatism (asymmetry and higher-order irregularity) out of the normal range [37].

Comparing irregular astigmatism between KC and PMD groups, PMD cases present with higher mean values for all Fourier parameters (▶ **Fig. 4**). The most reliable differentiating indicator between PMD and KC was found to be irregular astigmatism [37, 38].

Since the other ectatic corneal diseases, such as keratoglobus, posterior KC, and FTMD, demonstrate steeper curvatures, irregularities, and asymmetry, their pathology could also cause a significant disorientation in keratometric Fourier-derived parameters. Moreover, since these parameters could be evaluated for different zones and areas of the cornea, there is a strong conviction that they could be powerful indicators for the differential diagnosis among ectatic corneal diseases. However, no scientific studies examining these hypotheses have been established yet.

This document was downloaded for personal use only. Unauthorized distribution is strictly prohibited.

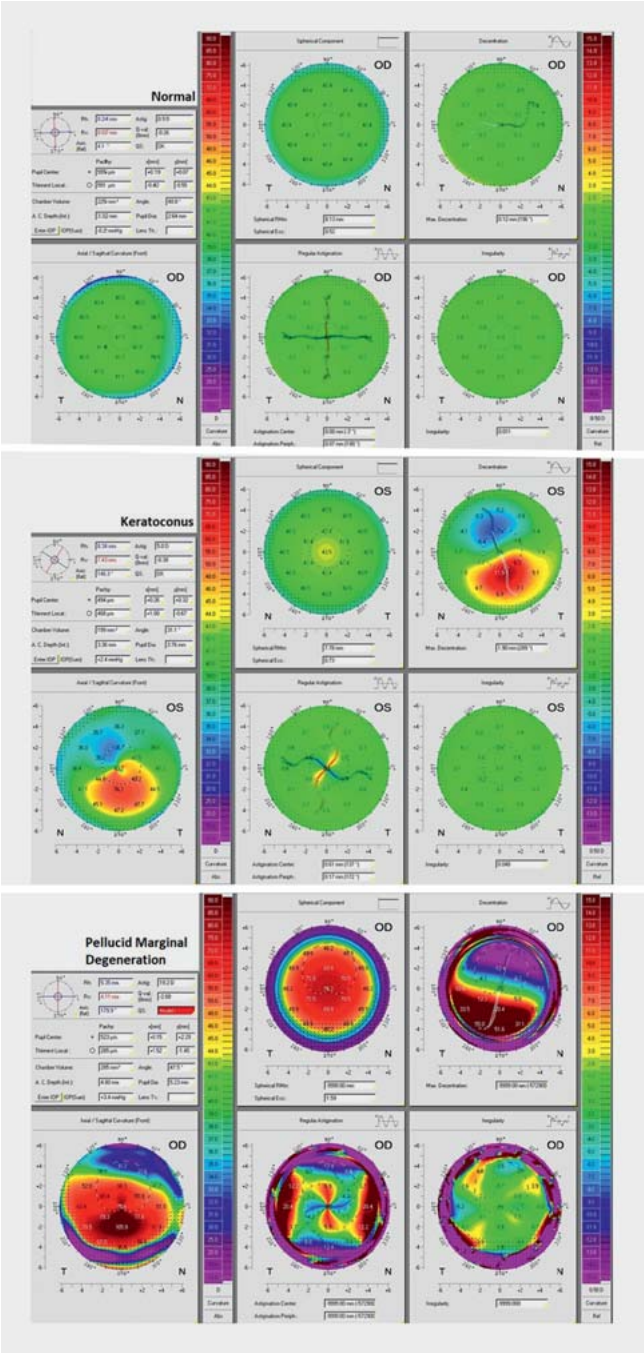

▶ **Fig. 4** Color-coded map for Fourier analysis in normal, keratoconus, and pellucid marginal degeneration patients.

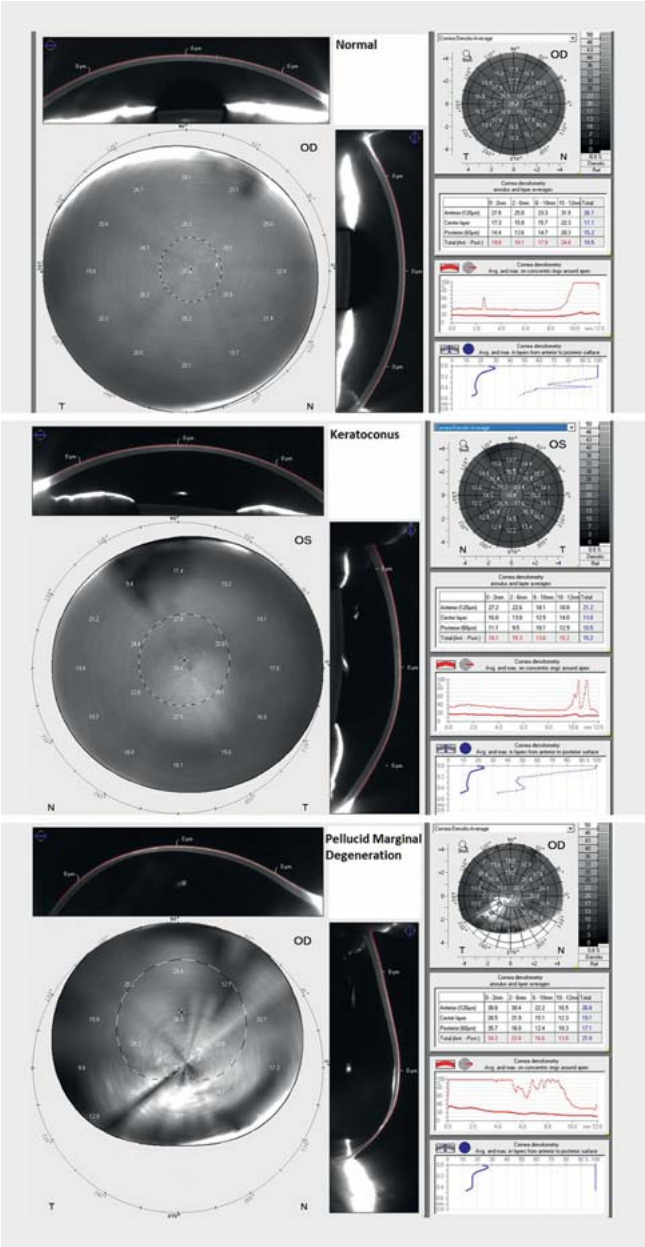

▶ **Fig. 5** Corneal densitometry display in the Pentacam in normal, keratoconus, and pellucid marginal degeneration patients.

Corneal optical densitometry

The cornea is a viscoelastic tissue with specific optical properties that result in corneal transparency in normal cases. Scheimpflug image analysis enables for structuring a map representing the amount of backscattered light in the different layers of the cornea. This is the most precise, accurate, and noninvasive method to document light scattering of the cornea. The software provides a standardized method of selective quantification of corneal opacities. The maximum and average corneal opacities are displayed in a color map. Opacities can also be viewed in selected layers. Corneal opacities are shown for defined annuli and depths, thus facilitating a uniform evaluation. It is also possible to compose a map of the amount of backscattered light in the different regions of the cornea, called a corneal densitometry map.

In KC, the structure of the cornea presents several changes caused by the ectatic nature of the disease (▶ **Fig. 5**). The fragile balance of the corneal extracellular matrix and cells is disrupted and for this reason, light scattering undergoes typical changes. Specifically, KC corneas present an increase in light backscattering in the central (0–2 mm, 2–6 mm in diameter) and total cornea. A higher densitometry in the central cornea was also reported in all

This document was downloaded for personal use only. Unauthorized distribution is strictly prohibited.

three layers examined by the software (anterior, central, and posterior) [39].

Furthermore, differences also exist between KC stages in corneal densitometry in view of the central annuli at total thickness, anterior, and central layers. More advanced cases presented a higher backscatter [39].

Although the corneal densitometry values have been found to be similar in the central 6 mm of the cornea in KC and PMD cases, the values were higher in PMD cases in the outermost area of the cornea from 6 to 12 mm (▸ **Fig. 5**). The difference was more significant in the 6–10 mm zone. The lower localization of corneal ectasia in PMD and its effect on the wider corneal area could be the reason for this difference. Therefore, a densitometric (6–12 mm zone) evaluation may add to the differential diagnosis [32].

The histopathological changes seen in keratoglobus, including the disruption of Bowman's layer and Descemet membrane breaks, would result in corneal hydrops and cause changes in corneal opacity. These alterations are very similar to those seen in advanced KC and the corneal optical densitometry measurements could also be similar. However, since these changes are located in different parts of the cornea, the location of corneal opacities could be a differential indicator among these two diseases. Unfortunately, there are no clinical studies available to confirm these approaches, yet.

The histopathology of posterior KC includes disorganization of the basal epithelium and basement membrane, fibrous replacement of Bowman's layer, thinned stroma with scarring, and irregular arrangements of central collagen lamellae. Moreover, variable structural changes in the Descemet membrane include thinning with small breaks, multilaminar configuration, abnormal anterior banding, and localized posterior excrescences [16]. All aforementioned alterations will change stromal clarity and could be identified using corneal optical densitometry. However, no studies have been released so far, yet, to confirm this hypothesis. As a peripheral thinning disorder with superficial vascularization and lipid deposition at the leading edge of the affected area, the transparency of the cornea in FTMD cases changes differently than in KC cases. Clinicians must expect the peripheral increase of corneal opacities in the corneal optical densitometry graph. However, there are no associated studies available.

Biomechanical properties

In the terminology of material science, the cornea is a complex anisotropic composite, with nonlinear elastic and viscoelastic properties. Viscoelastic materials, as their name suggests, combine two different properties. The term "viscous" implies that they deform slowly when exposed to an external force. The term "elastic" implies that once a deforming force has been removed, the material will return to its original configuration. In practice, this means that elastic material instantaneously returns to its original shape after a force is removed whereas viscoelastic materials present a time-dependent response. As opposed to the symmetric loading and unloading behavior of purely elastic materials, viscoelastic materials return to their pre-stress configuration via different stress–strain pathways that depend on loading rates. This discordance between loading and unloading behavior can be partially characterized by "hysteresis".

The cornea is such a complex biomechanical composite because it consists of different structural layers with different organization patterns. The Bowman's layer and the stroma, which are the only collagenous layers, provide the main corneal tensile strength. The epithelium has a limited effect on tensile strength, and its removal causes little or no change in the overall biomechanical behavior. Descemet membrane has extensibility and low stiffness that ensures the laxity over a broad range of intraocular pressures (IOPs) and may serve as a high-compliance buffer to protect the endothelium from the effects of high stromal stresses [40].

The biomechanical properties of the cornea can be measured by the evaluation of the corneal response to a mechanical stress stimulus. This can be achieved by an external force such as an air pulse. Pioneer implementation equipment provides a combination of an air pulse tonometer with an ultrahigh-speed Scheimpflug camera. The ocular response analyzer (ORA; Reichert Ophthalmic Instruments, Inc., Buffalo, NY, USA) and the Corvis ST (Oculus; Wetzlar, Germany) are two commercially available instruments based on these principles. An air pulse is released, and a high-speed camera tracks the biomechanical response of the cornea. The movement of the cornea is mainly influenced by the IOP, biomechanical properties of the cornea, and corneal thickness.

At the beginning, the cornea is in its initial convex shape. The air pulse drives the cornea backwards until the first applanation occurs. Afterwards, the cornea is further deformed until the moment of maximal concavity. After an oscillation phase, the cornea returns to its original shape. Before it reaches the initial state, it passes through a second applanation, with a second flattening of the cornea. During this dynamic corneal response, three moments in time are of major interest.

- The first applanation, when the cornea is flat.
- The moment of highest concavity.
- The second applanation, when the cornea is flat again, before it returns to its original state.

During the whole process, several biomechanical dynamic corneal response parameters are recorded. ORA provides the following parameters: (1) corneal hysteresis (CH), which quantifies the dynamics of corneal deformation and recovery, (2) corneal resistance factor (CRF), which is proposed to be a measure of the elastic resistance of the cornea, (3) the keratoconus match index (KMI), which represents the similarity of the waveform of the examined eye against the same average waveform scores of the keratoconic eyes in the machine's database, and (4) the keratoconus match probability (KMP), which attempts to quantify the probability that a certain eye is normal, suspect, or keratoconic.

The Corvis ST provides the Corvis biomechanical index (CBI), which is designed to detect early KC based on the biomechanical response of the cornea and includes several dynamic corneal response parameters such as deformation amplitude ratio at the center and 2 mm, applanation 1 velocity, integrated radius, Ambrósio's relational thickness to the horizontal profile, and a novel stiffness parameter (SP-A1; ▸ **Fig. 6**).

Moreover, there are several other parameters related to the dynamic corneal response, corneal stiffness, and the stress–strain response [40, 41].

This document was downloaded for personal use only. Unauthorized distribution is strictly prohibited.

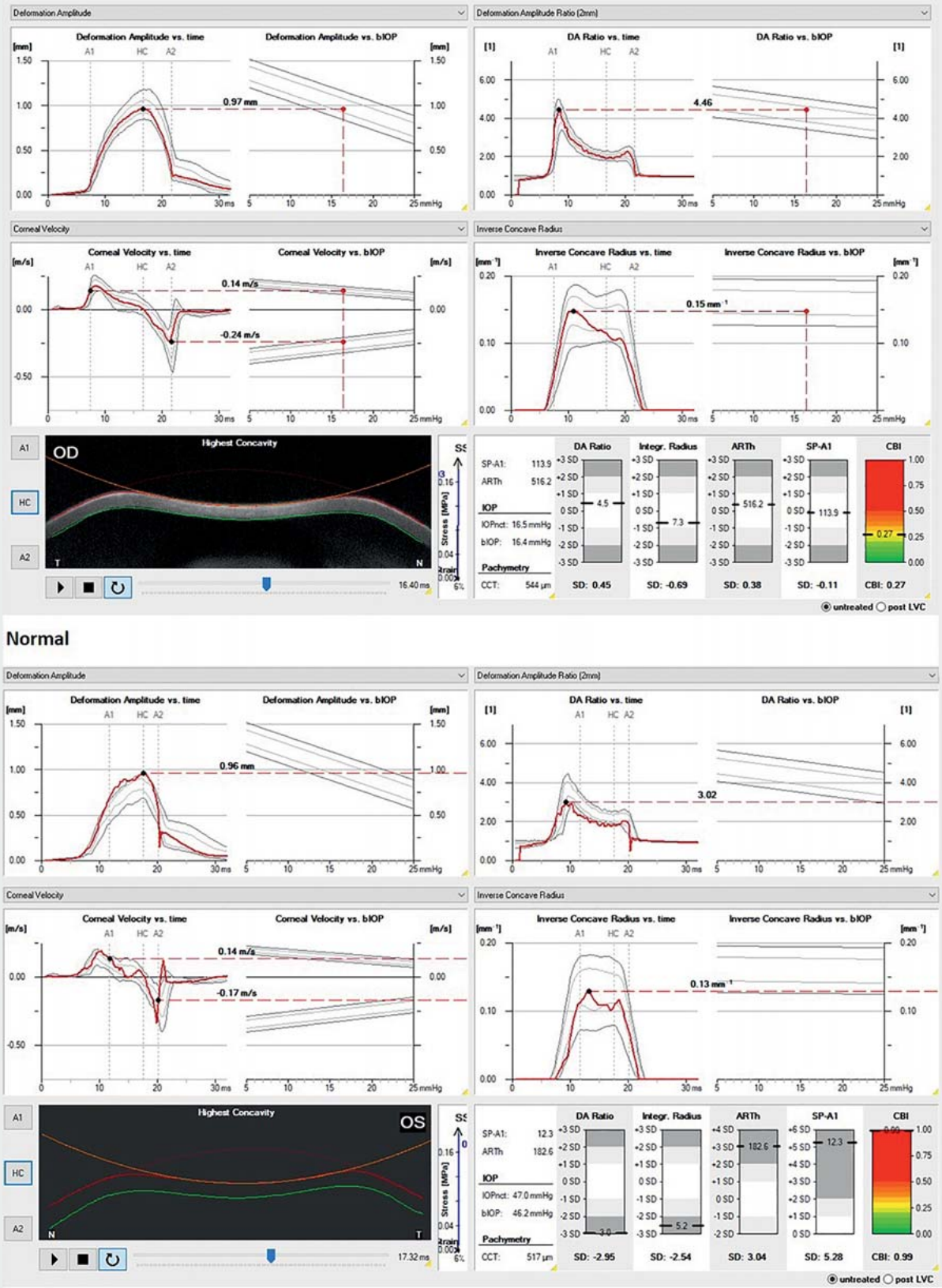

▶ **Fig. 6** The Corvis ST parameters in normal and keratoconus patients.

This document was downloaded for personal use only. Unauthorized distribution is strictly prohibited.

Prior to corneal curvature or thickness change due to the disease, the corneal stiffness and elasticity is already altered. Therefore, the measurement of biomechanical properties is crucial for the detection of subclinical cases, staging, and differential diagnosis [40–44].

Most of the aforementioned parameters indicated that the biomechanical properties of normal and keratoconic eyes were significantly different [43–45]. Consequently, there is the assumption of a significantly smaller deformation of the central cornea in PMD corneas than in healthy corneas [46]. Biomechanical parameters obtained from ORA in PMD cases were found to be statistically significantly lower than in normal eyes [46]. The Corvis software indicated that only the maximum deformation amplitude and the time from the start until the second applanation was statistically different between PMD and healthy corneas [44]. Moreover, 11 Corvis parameters were found to be different between KC and PMD, which is probably because the Corvis measures in the corneal center, which rarely changes in PMD [46]. Therefore, it seems to be suitable to analyze the biomechanical properties of the inferior cornea in PMD corneas instead of the central cornea, but there is no *in vivo* measurement that could analyze a specific corneal area. ORA and Corvis mainly evaluate the center of the cornea and provide an overall biomechanical response.

Different corneal biomechanical properties may be expected due to different positions of the corneal apex relative to the pupil entrance and different locations of structural changes observed in PMD corneas compared to KC. Increased corneal resistance could arise because of the redistribution of collagen fibers. Another hypothesis is that interlamellar and interfibrillar slippage lead to the local thinning of KC corneas. Particularly in KC, orthogonal collagen fibers can slip; thus, slipping of the circumferential limbal collagen in PMD is conceivable. Nevertheless, CH and CRF were close to those found in the KC group and cannot be used as a diagnostic factor in distinguishing between PMD and KC [47].

In keratoglobus, FTMD, and KC posticus generalis, the thinning area affects different corneal areas compared to KC. Therefore, a different biomechanical response could be expected among them. However, until now, there are no studies available to prove that.

Confocal microscopy

Confocal microscopy studies showed that corneal cell morphology in KC varies significantly from that in healthy eyes. Furthermore, there was a KC stage-dependent difference in morphological alterations, which is suggestive of progressive cellular changes in the cornea during the progression of the disease. Qualitatively, studies demonstrated enlarged basal epithelial cells, structural changes in sub-basal and stromal nerve fibers, abnormal stromal keratocytes and keratocyte nuclei, and pleomorphism and enlargement of endothelial cells. Quantitatively, when compared with control corneas, significant reductions in basal epithelial cell density, anterior stromal keratocyte density, posterior stromal keratocyte density, endothelial cell density, sub-basal nerve fiber density, sub-basal nerve fiber length, and sub-basal nerve branch density were observed in KC corneas [48]. Recently, corneal confocal microscopy visualized slightest alterations within the corneal sub-basal nerve plexus in KC including (a) a significantly lower corneal nerve fiber length and (b) an enhanced winding course of the sub-basal nerve plexus [49].

Normal morphologic features in the central cornea were observed in PMD corneas, whereas irregular and elongated epithelial cells with an altered arrangement of keratocytes were found in peripheral sections [50].

The morphological changes of the cornea with ocular *in vivo* confocal microscopy in patients with FTMD have been studied previously. Compared to healthy controls, the corneal epithelial and endothelial cells in the FTMD group showed granular highly reflective substances and thinner subepithelial nerve fibers. The uneven dot-like highly reflective substances without cell structures appeared in the stromal layer of the cornea. The density of central and marginal corneal epithelial cells, stromal cells, and subepithelial nerve fibers was lower in the FTMD group, and they were negatively correlated with the severity of the disease. Moreover, the density of corneal epithelial cells, stromal cells, and sensory plexus nerve fibers was significantly reduced in the FTMD group. The pathological changes were more obvious in the marginal cornea, and they correlated with the severity of the disease [51]. This difference between the central and the marginal cornea might be a differential factor between FTMD and KC.

Corneal epithelial thickness

Knowledge of the distribution of ET may be beneficial in close-call clinical judgments and can aid in diagnosing ectatic diseases. The reason for this is that the epithelium is not of homogeneous depth over the Bowman layer. Often, the epithelium compensates for stromal surface irregularities, becoming thicker over flat areas and thinner over steep areas, where the stroma protrudes. In other words, the epithelium attempts to minimize abrupt changes in stromal thickness. As a result, the anterior cornea may project a smoother topography and more regular wavefront error map in comparison with the underlying anterior stroma. ET can be measured noninvasively and with high accuracy by spatial domain AS-OCT. In normal corneas, ET consists of 5–7 cell layers and has an average central thickness ranging from 50 to 52 µm [52–54]. Compared to normal corneas, KC corneas did not have differences in central ET [52, 53]. However, KC is associated with a doughnut pattern, an inferior thinning pattern, and a max–min ET increasement [52, 54]. Moreover, the difference between superior ET and inferior ET was found to be positive in KC patients and negative in control groups [53]. PMD, as expected, presented no changes in central ET but a thinning in a band-like shape adjusted to the inferior corneal limbus [55]. Interestingly, Mohr et al. detected ET thinning in the inferior periphery in PMD, where the epithelium would be expected to be thicker in a healthy population. Compared to KC corneas, the first main difference was found in the inferior 7–9 mm sector, where ET was lower in PMD eyes. Additionally, ET was also lower in PMD eyes in the adjacent inferotemporal 7–9 mm sector. The second major difference was detected in the inferotemporal 2–5 mm sector, which in turn exhibited a lower ET in the KC group. Furthermore, KC eyes showed significantly lower ET readings in the inferior 2–5 mm sector [55]. No reports were found in the literature concerning the ET in keratoglobus, posterior KC, and FTMD.

This document was downloaded for personal use only. Unauthorized distribution is strictly prohibited.

▶ **Table 4** Main distinct clinical features between keratoconus and keratoconus-related diseases.

Differential factors	Keratoconus	Pellucid marginal degeneration	Keratoglobus	Posterior keratoconus	Fuchs-Terrien marginal degeneration
Slit lamp	▪ Fleischer ring ▪ Vogt striae ▪ Bowman layer scarring ▪ Posterior and anterior corneal protrusion	▪ Lack of Fleischer ring, Vogt striae, and scarring	▪ Lack of Fleischer ring, Vogt striae, and scarring	▪ Posterior corneal protrusion ▪ Intact anterior cornea	▪ Superior thinning ▪ Peripheral lipid deposition and vascularization
Topography and tomography	▪ Central, inferior steepening	▪ Crab claw, inferior steepening ▪ Against-the-rule astigmatism	▪ Whole cornea steepening ▪ Peripheral arc of increased power	▪ Keratoconus posticus generalis: Uniform posterior corneal steepening ▪ Keratoconus posticus circumscriptus: superior, nasal, temporal, or inferior steepening	▪ Flattening of vertical meridian ▪ Characteristic “against-the-rule” astigmatism
Pachymetric data	▪ Central or inferior paracentral thinning	▪ Higher mean CCT and TCP values ▪ Significant inferior location of TCP	▪ Diffuse and extensive thinning ▪ Globular protrusion	▪ Keratoconus posticus generalis: diffuse thinning of the entire corneal surface ▪ Keratoconus posticus circumscriptus: central or paracentral thinning	▪ Superior thinning ▪ Circumferential peripheral thinning (if advanced)
Elevation maps	▪ Central or inferior maximum elevation point ▪ Asymmetric island pattern ▪ Asymmetric regular ridge ▪ Central island	▪ Higher maximum elevation ▪ Inferior maximum elevation point ▪ Asymmetric island pattern	▪ High values in total anterior and posterior corneal area	▪ Normal anterior elevation map	▪ Superotemporal paracentral maximum elevation point
Biomechanical properties	▪ Altered biomechanical properties compared to normal	▪ Different biomechanical response could be expected due to different affected areas ▪ Corvis biomechanical parameters were higher	▪ Different biomechanical response could be expected due to different affected area and differences in corneal structure		
HOAs	▪ Higher anterior corneal HOAs compared to normal ▪ Negative values of spherical aberration	▪ Higher degree of trefoil ▪ Positive value of spherical aberration	▪ Different HOAs profiles could be expected due to different corneal tomography characteristics and wavefronts		
Fourier analysis	▪ Higher keratometric Fourier parameters compared to normal	▪ Higher mean values of irregular astigmatism	▪ Significant disorientation of keratometric Fourier derived parameters could be expected due to different topographic characteristics		
Corneal optical densitometry	▪ Increased back scattered light compared to normal	▪ Higher backscattered light in the outermost area of the cornea	▪ Different location and values of backscattered light could be expected due to different location of affected area and corneal structure		

continued

This document was downloaded for personal use only. Unauthorized distribution is strictly prohibited.

▶ **Table 4** *Continued*

Differential factors	Keratoconus	Pellucid marginal degeneration	Keratoglobus	Posterior keratoconus	Fuchs-Terrien marginal degeneration
Confocal microscopy	Significant reductions in ▪ basal epithelial cell density ▪ anterior stromal keratocyte density ▪ posterior stromal keratocyte density ▪ endothelial cell density ▪ sub-basal nerve fiber density ▪ sub-basal nerve fiber length ▪ sub-basal nerve branch density ▪ corneal nerve fiber length ▪ an enhanced winding course of the sub-basal nerve plexus	▪ Normal morphologic features in the central cornea ▪ Irregular and elongated epithelial cells with altered arrangement of keratocytes in peripheral sections	▪ No confocal microscopy for keratoglobus and posterior keratoconus cases available		Significant reduction in ▪ density of corneal epithelial cells ▪ density of stromal cells ▪ sensory plexus nerve fibers more obvious in the marginal cornea
Epithelial thickness	▪ No differences in central ET ▪ Doughnut pattern in ET maps ▪ Inferior thinning pattern in ET maps ▪ Max–min ET increasement ▪ Positive superior-inferior ET difference compared to normal	▪ No differences in central ET ▪ Thinning in a band-like shape adjusted to the inferior corneal limbus Interestingly ▪ Thinning in the inferior periphery in PMD compared to normal ▪ Lower ET in the inferior and inferotemporal peripheral corneal sectors (7–9 mm) ▪ Higher ET in the inferior and inferotemporal paracentral corneal sectors (2–5 mm)	No ET reports for keratoglobus, posterior Keratoconus, and Fuchs-Terrien marginal degeneration		

CCT: central corneal thickness, TCP: thinnest corneal pachymetry, HOAs: higher-order aberrations, ET: epithelial thickness

This document was downloaded for personal use only. Unauthorized distribution is strictly prohibited.

Summary

KC is manifested by progressive corneal thinning, protrusion, and scarring, resulting in distorted and decreased vision. Primary non-inflammatory corneal thinning disorders that mimic KC are PMD, keratoglobus, posterior KC, and FTMD. These disorders may represent varied clinical features based on the underlying abnormality. Nowadays, pioneer instrumentation enables and ensures the differentiation between the different ectatic corneal diseases. Summarized main distinct clinical features between KC and KC-related diseases are presented in ▶ **Table 4**.

Acknowledgements

We would like to thank Ms Christina Turner for the linguistic revision and corrections of the manuscript.

Conflict of Interest

The authors declare that they have no conflict of interest.

References

[1] Rabinowitz YS. Keratoconus. Surv Ophthalmol 1998; 42: 297–319. doi:10.1016/s0039-6257(97)00119-7

[2] Shakir O. Stromal Degenerations. In: Schmidt-Erfurth U, Kohnen T, eds. Encyclopedia of Ophthalmology. Berlin, Heidelberg: Springer; 2018: 931–939

[3] Ertan A, Muftuoglu O. Keratoconus clinical findings according to different age and gender groups. Cornea 2008; 27: 1109–1113. doi:10.1097/ICO.0b013e31817f815a

[4] Gokhale NS. Epidemiology of keratoconus. Indian J Ophthalmol 2013; 61: 382–383. doi:10.4103/0301-4738.116054

[5] Kennedy RH, Bourne WM, Dyer JA. A 48-year clinical and epidemiologic study of keratoconus. Am J Ophthalmol 1986; 101: 267–273. doi:10.1016/0002-9394(86)90817-2

[6] Flockerzi E, Xanthopoulou K, Goebels SC et al. Keratoconus staging by decades: a baseline ABCD classification of 1000 patients in the Homburg Keratoconus Center. Br J Ophthalmol 2021; 105: 1069–1075. doi:10.1136/bjophthalmol-2020-316789.

[7] Krachmer JH. Pellucid marginal corneal degeneration. Arch Ophthalmol 1978; 96: 1217–1221

[8] Stankovic I, Stankovic M. Ein Beitrag zur Kenntnis des Keratotorus. Klin Monbl Augenheilkd 1966; 148: 873–879

[9] Zucchini G. Su di un case di degenerazione marginale della cornea – varieta inferiore pellucida – studio clinic ed istologico. Ann Ottalmol Clin Oculitl 1962; 88: 47–56

[10] Nelson ME, Talbot JF. Keratoglobus in Rubinstein-Taybi syndrome. Br J Ophthalmol 1989; 73: 385–387. doi:10.1136/bjo.73.5.385

[11] Biglan AW, Brown SI, Johnson BL. Keratoglobus and blue sclera. Am J Ophthalmol 1977; 83: 225–233. doi:10.1016/0002-9394(77)90621-3

[12] Meghpara B, Nakamura H, Vemuganti G et al. Histopathologic and immunohistochemical studies of keratoglobus. Arch Ophthalmol 2009; 127: 1029–1035. doi:10.1001/archophthalmol.2009.184

[13] Perkins ES. Myopia and scleral stress. Doc Ophthalmol Proc Series 1981; 28: 121–127. doi:10.1007/978-94-009-8662-6_18

[14] Butler TH. Two Rare Corneal Conditions: I. Acute Conical Corneal II. Posticus Circumscriptus. Br J Ophthalmol 1932; 16: 30–35. doi:10.1136/bjo.16.1.30

[15] Silas M, Hilkert S, Reidy J et al. Posterior keratoconus. Br J Ophthalmol 2018; 102: 863–867. doi:10.1136/bjophthalmol-2017-311097

[16] Krachmer JH, Rodrigues MM. Posterior keratoconus. Arch Ophthalmol 1978; 96: 1867–1873. doi:10.1001/archopht.1978.03910060371016.

[17] Süveges I, Levai G, Alberth B. Pathology of Terrien's Disease. Histochemical and electron microscopic study. Am J Ophthalmol 1972; 74: 1191–1200. doi:10.1016/0002-9394(72)90742-8

[18] Chan AT, Ulate R, Goldich Y et al. Terrien Marginal Degeneration. Clinical Characteristics and Outcomes. Am J Ophthalmol 2015; 160: 867–872. doi:10.1016/j.ajo.2016.01.001

[19] Zarei-Ghanavati S, Javadi MA, Yazdani S. Bilateral Terrien's Marginal Degeneration and Posterior Polymorphous Dystrophy in a Patient with Rheumatoid Arthritis. J Ophthalmic Vis Res 2012; 7: 60–63

[20] Imbornoni LM, McGhee CNJ, Belin MW. Evolution of keratoconus: from the diagnosis to therapeutics. Klin Monbl Augenheilkd 2018; 235: 680–688. doi:10.1055/s-0044-100617

[21] Ross JV. Keratoconus posticus generalis. Am J Ophthalmol 1950; 33: 801–803. doi:10.1016/0002-9394(50)90210-8

[22] Belin MW, Asota IM, Ambrosio R jr. et al. What's in a name: keratoconus, pellucid marginal degeneration, and related thinning disorders. Am J Ophthalmol 2011; 152: 157–162. doi:10.1016/j.ajo.2011.03.028

[23] Fuchihata M, Maeda N, Toda R et al. Characteristics of corneal topographic and pachymetric patterns in patients with pellucid marginal corneal degeneration. Jpn J Ophthalmol 2013; 58: 131–138. doi:10.1007/s10384-013-0291-3

[24] Koçluk Y, Yalnoz-Akkaya Z, Burcu A et al. Comparison of Scheimpflug imaging analysis of pellucid marginal corneal degeneration and keratoconus. Ophthalmic Res 2015; 53: 21–27. doi:10.1159/000365518

[25] Wallang BS, Das S. Keratoglobus. Eye (Lond) 2013; 27: 1004–1012. doi:10.1038/eye.2013.130

[26] Rao S, Padmanabhan P. Posterior keratoconus. An expanded classification scheme based on corneal topography. Ophthalmology 1998; 105: 1206–1212. doi:10.1016/S0161-6420(98)97022-1

[27] Tummanapalli SS, Maseedupally V, Mandathara P et al. Evaluation of corneal elevation and thickness indices in pellucid marginal degeneration and keratoconus. J Cataract Refract Surg 2013; 39: 56–65. doi:10.1016/j.jcrs.2012.08.053

[28] Martinez-Abad A, Pinero D. Pellucid marginal degeneration: Detection, discrimination from other corneal ectatic disorders and progression. Cont Lens Anterior Eye 2019; 42: 341–349. doi:10.1016/j.clae.2018.11.010

[29] Pircher N, Lammer J, Holzer S et al. Corneal crosslinking for pellucid marginal degeneration. J Cataract Refract Surg 2019; 45: 1163–1167. doi:10.1016/j.jcrs.2019.03.018

[30] Piñero DP, Nieto JC, Lopez-Miguel A. Characterization of corneal structure in keratoconus. J Cataract Refract Surg 2012; 38: 2167–2183. doi:10.1016/j.jcrs.2012.10.022

[31] Sideroudi H, Labiris G, Giarmoukakis A et al. Contribution of reference bodies in diagnosis of keratoconus. Optom Vis Sci 2014; 91: 676–681. doi:10.1097/OPX.0000000000000258

[32] Koc M, Tekin K, Inanc M et al. Crab claw pattern on corneal topography: pellucid marginal degeneration or inferior keratoconus? Eye (Lond) 2018; 32: 11–18. doi:10.1038/eye.2017.198

[33] Piñero DP, Alió JL, Alesón A et al. Pentacam posterior and anterior corneal aberrations in normal and keratoconic eyes. Clin Exp Optom 2009; 92: 297–303. doi:10.1111/j.1444-0938.2009.00357.x

[34] Oie Y, Maeda N, Kosaki R et al. Characteristics of ocular higher order aberrations in patients with pellucid marginal corneal degeneration. J Cataract Refract Surg 2008; 34: 1928–1934. doi:10.1016/j.jcrs.2008.06.038

[35] Sideroudi H, Labiris G, Georgatzoglou K et al. Fourier analysis of videokeratography data. Clinical usefulness in grade I and subclinical kerato-

This document was downloaded for personal use only. Unauthorized distribution is strictly prohibited.

conus. J Cataract Refract Surg 2016; 42: 731–737. doi:10.1016/j.jcrs.2016.01.049

[36] Sideroudi H, Labiris G, Georgantzoglou K et al. Fourier analysis algorithm for the posterior corneal keratometric data. Clinical usefulness in keratoconus. Ophthalmic Physiol Opt 2017; 37: 460–466. doi:10.1111/opo.12386

[37] Grünauer-Kloevekorn C, Fischer U, Kloevekorn-Norgall K et al. Pellucid marginal corneal degeneration. Evaluation of the corneal surface and contact lens fitting. Br J Ophthalmol 2006; 90: 318–323. doi:10.1136/bjo.2005.079988

[38] Grünauer-Kloevekorn C, Kloevekorn-Fischer U, Kloevekorn-Norgall K et al. [Quantitative assessment of topographical parameters to differentiate keratoconus from pellucid marginal corneal degeneration. Klin Monbl Augenheilkd 2005; 222: 874–882. doi:10.1055/s-2005-858822

[39] Lopes B, Ramos I, Ambrósio R Jr. Corneal densitometry in keratoconus. Cornea 2014; 33: 1282–1286. doi:10.1097/ICO.0000000000000266

[40] Gatzioufas Z, Seitz B. [New aspects on biomechanics of the cornea in keratoconus]. Ophthalmologe 2013; 110: 812–817. doi:10.1007/s00347-013-2818-x

[41] Ren S, Xu L, Fan Q et al. Accuracy of new Corvis ST parameters for detecting subclinical and clinical keratoconus eyes in a Chinese population. Sci Rep 2021; 11: 4962–4972. doi:10.1038/s41598-021-84370-y

[42] Flockerzi E, Häfner L, Xanthopoulou K et al. Reliability analysis of successive Corneal Visualization Scheimpflug Technology measurements in different keratoconus stages. Acta Ophthalmol 2022; 100: e83–e90. doi:10.1111/aos.14857

[43] Flockerzi E, Vinciguerra R, Belin MW et al. Combined biomechanical and tomographic keratoconus staging: Adding a biomechanical parameter to the ABCD keratoconus staging system. Acta Ophthalmol 2022; 100: e1135–e1142. doi:10.1111/aos.15044

[44] Labiris G, Giarmoukakis A, Gatzioufas Z et al. Diagnostic capacity of the keratoconus match index and keratoconus match probability in subclinical keratoconus. J Cataract Refract Surg 2014; 40: 999–1005. doi:10.1016/j.jcrs.2013.08.064

[45] Elham R, Jafarzadehpur E, Hashemi H et al. Keratoconus diagnosis using Corvis ST measured biomechanical parameters. J Curr Ophthalmol 2017; 29: 175–181. doi:10.1016/j.joco.2017.05.002

[46] Labiris G, Giarmoukakis A, Sideroudi H et al. Diagnostic capacity of biomechanical indices from a dynamic bidirectional applanation device in pellucid marginal degeneration. J Cataract Refract Surg 2014; 40: 1006–1012. doi:10.1016/j.jcrs.2014.03.018

[47] Sedaghat MR, Ostadi-Maghadam H, Jabbarvand M et al. Corneal hysteresis and corneal resistance factor in pellucid marginal degeneration. J Curr Ophthalmol 2017; 30: 42–47. doi:10.1016/j.joco.2017.08.002

[48] Uçakhan OO, Kanpolat A, Ylmaz N et al. *In vivo* confocal microscopy findings in keratoconus. Eye Contact Lens 2006; 32: 183–191. doi:10.1097/01.icl.0000189038.74139.4a

[49] Flockerzi E, Daas L, Seitz B. Structural changes in the corneal nerve plexus in keratoconus. Acta Ophthalmol 2020; 98: 928–932. doi:10.1111/aos.14432

[50] Di Silvestre L, Mularoni A, Casamenti V et al. Cornea in Pellucid Marginal Degeneration: *In vivo* Confocal Microscopy Analysis Before and After the Treatment with Intra Corneal Ring (ICR). IOVS2005; 46: 2719

[51] Chen T, Li Q, Tang X et al. *In Vivo* Confocal Microscopy of Cornea in Patients with Terrien's Marginal Corneal Degeneration. J Ophthalmol 2019; 2019: 1–8. doi:10.1155/2019/3161843

[52] Levy A, Georgeon C, Knoeri J et al. Corneal Epithelial Thickness Mapping in the Diagnosis of Ocular Surface Disorders Involving the Corneal Epithelium: A Comparative Study. Cornea 2022. doi:10.1097/ICO.0000000000003012

[53] Lahme L, Storp JJ, Diener R et al. [Corneal epithelial thickness in keratoconus patients compared to healthy controls]. Ophthalmologe 2022. doi:10.1007/s00347-022-01606-6

[54] Serrao S, Lombardo G, Calì C, Lombardo M. Role of corneal epithelial thickness mapping in the evaluation of keratoconus. Cont Lens Anterior Eye 2019; 42: 662–665. doi:10.1016/j.clae.2019.04.019

[55] Mohr N, Shajari M, Krause D et al. Pellucid marginal degeneration versus keratoconus: distinction with wide-field SD-OCT corneal sublayer pachymetry. Br J Ophthalmol 2021; 105: 1638–1644. doi:10.1136/bjophthalmol-2020-316496

This document was downloaded for personal use only. Unauthorized distribution is strictly prohibited.